A metrological device for robot identification

Sebastien Garnier, Kévin Subrin

Version of Record: https://www.sciencedirect.com/science/article/pii/S0736584521001290
Manuscript_695028406336af48f7512e6c294dba92

A metrological device for robot identification

Sebastien Garnier[a], Kevin Subrin[a]

[a]Associate Professor, Department of Mechanical Engineering, Laboratory of Digital Sciences of Nantes, IUT of Nantes, University of Nantes France

ARTICLE INFO

Keywords:
Industrial Robot
Elasto-static behavior
stiffness analysis
Design methodology

ABSTRACT

Nowadays, industrial robots are increasingly used for heavy manufacturing tasks such as milling, drilling, deburring or sanding. Twenty years ago, researchers began to identify scientific bottlenecks and have made contributions on robot performance in terms of repeatability and accuracy. We are currently observing many methods and tools to apply to improve robot performances through their geometric, kinematic and dynamic modelling. There are often laboratory tools, not compatible with the needs of companies i.e. economically compatible, easy to install, easy to use with a good integration to industrial lines. In this context, we propose a new device to identify robot performances based on the famous ballbar used for the calibration of machine-tools. This paper thus deals with the design methodology, its design and environment of use as well as its performance in robot identification.

1. Introduction

Nowadays, industrial robots are increasingly used for tasks that require accuracy. With the development of technology, robot manufacturers are offering both proprioceptive systems for path control such as force sensor or double encoding actuators. There are also exteroceptive systems such as high-speed cameras that, after calibration, allow precise robot positioning. However, in manufacturing environments where tasks are subject to stress with large fluctuations in force (e.g. machining), the implementation of geometric, kinematic or even dynamic models is a must to improve robot accuracy [1]. These models involve a set of parameters that need to be identified : lengths between the robot joints, apparent stiffness, moving masses, inertia, friction or backlashes. Designing a new metrological tool to improve robot performances through parameters identification must reply to the industry need.
Nowadays, literature performs identification with an expensive tool such as laser tracker ([2],[3],[4],[5],[6],[7]) but to identify heavy robots with large workspace, this approach is questionable : comparing robot accuracy (around 1mm), robot repeatability (around 0.1mm), is a metrological tool accuracy of 0.005mm pertinent ? Moreover, its implementation is often cumbersome and costly: robot immobilization for a few days, definition of postures where the targets are visible by the laser tracker, definition of postures in accordance with the literature, definition of working reference points, geometric identification and finally elastostatic (with and without mass) [2]. Constructing a real loop of measurement offers advantages being closer to the system to measure but its integration is a key to facilitate its use.
The novelty of this article concerns the design of a patented metrological measuring system based on the principle of a machine tool ballbar. The article is structured as follows. Section 2 reviews the measuring systems and methods to apply a wrench. Section 3 focuses on a technical approach to define the specifications and presents the system. Section 4 focuses on the analysis, the identification and the performances of the system. The conclusion and the perspectives are finally discussed.

2. Systems and methods review to identify robots behavior

2.1. Current approaches

The evolution of robotic systems is the result of improvements involving the fields of mechanics, electronics and control. Indeed, over the last thirty years, robots have evolved through new mechanical architectures (serial, parallel, hybrid robot), with increasingly advanced drive technologies (Harmonic drive [8], double-encoding actuators [9], gravity compensator [10]) allowing compactness and improving accuracy while limiting backlashes [11]. However,

*Kevin Subrin
sebastien.garnier@ls2n.fr (S. Garnier); kevin.subrin@ls2n.fr (.K. Subrin)
ORCID(s):

these evolutions are accompanied by improvements in terms of control to identify friction and ensure a stable behavior of the robot [12]. The measurement of robot performance is based on the following protocols namely : ISO 9283:1998 about Industrial Robots - Performance Criteria and Related Test Methods [13]. It addresses the one-directional pose accuracy and repeatability measuring the difference between the position reached and the position controlled in terms of average deviation and maximum dispersion (Fig. 1).

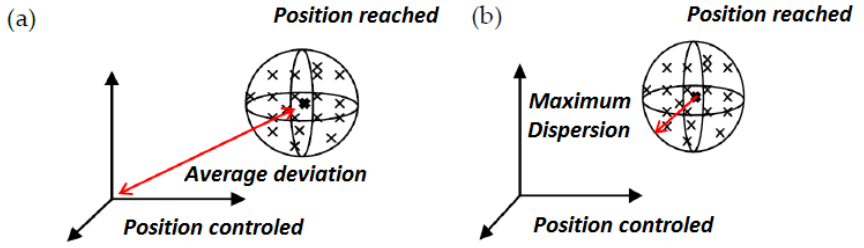

Figure 1: Accuracy (a) and repeatability (b) according ISO 9283:1998

The measuring equipment is not specified in this norm and literature provides many equipments to characterize the robot performance. Laser tracker is generally used as it provides an accuracy (depending on the distance to be measured) of several μm in a workspace of several m^3 or to compare the performance of new equipment. Understanding the deflection of the robot under stress requires the implementation of a stress such as an associated mass [2], a pneumatic system [14] or an electrical system with cables [6] allowing the transmission of the forces associated with a measuring device to be synchronized. The Tab. 1 lists the works carried out in this field underlying the equipment used, the protocol, the device and the information extracted from the measurements. The Fig. 2 highlights the implementation.

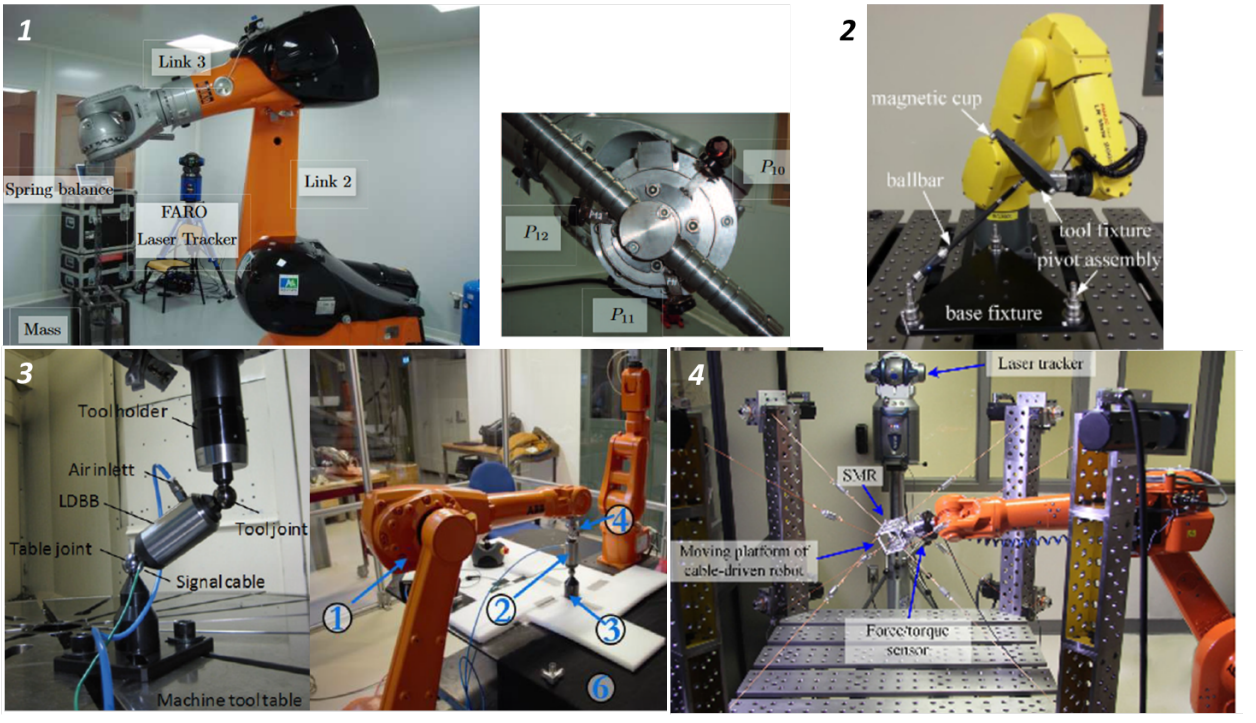

Figure 2: Dedicated system to evaluate the elastostatic parameters. In 1, method with a weigth [18]; in 2, method with a ballbar [15]; in 3, Loaded Double Ball Bar [14]; in 4, method with a cable driven parallel robot [6]

References	Measurement	Identification Methodology
Dumas et al. 2011 [2]	Weight and Tracker	Complete pose method (3 positions and 3 orientations) with 2 steps to determine the 5 last articular stiffness and the first one. See Fig.2.1
Guerin et al. 2014 [7]	Weight and Tracker	Partial Pose Method (3 positions) to identify a 6 Degrees of Freedom industrial robot located on a track
Nubiola et al. 2014 [15]	Ballbar	One fixture is attached to the robot base and the other to the robot end-effector, and each having three magnetic cups. 72 poses of the tool fixture, with respect to the base fixture, it is possible to measure six distances with the ballbar between the magnetic cups on the tool fixture and the magnetic cups on the base fixture, and thus calculate the pose with high accuracy. See Fig. 2.2
Nubiola et al. 2014 [16]	Optical CMM (Coordinate Measuring Machines) compared to Laser tracker	A laser tracker and an optical CMM are compared to evaluate a full kinematic calibration and compliance parameters relative to joint stiffness.
Theissen et al. 2014 [4]	Double Loading Ballbar [14] + Tracker	The measuring methodology utilizes the Double Loading Ball Bar to customize wrench vectors and a laser tracker to measure the system response. In particular, the Double Loading Ball Bar creates the closed-force-loop to create a flow of forces similar to the intended application of the robot. See Fig. 2.3
Wu et al. 2015 [5]	Weight and Tracker	it mainly focuses on the methodology i.e. Partial pose method (3 positions)
Ambiehl et al. 2017 [3]	Weight et tracker	Elasto-static identification : comparison between 3 approaches : complete Pose method (3 positions and 3 orientations), Partial pose method (3 positions) and Decoupled partial pose where the 3 first joint are identified in an independant way than the 3 last one
Filion et al. 2018 [17]	Portable photogrammetry system is compared to Laser tracker	A portable photogrammetry system (the MaxSHOT 3D) compared with a laser tracker (the FARO laser tracker) to improve robot position accuracy
Kamali et al. 2019 [6]	Cable Driven Parallel Robot and tracker	Setup includes a parallel cable-driven mechanism for applying loads and a laser tracker for measuring the tool center point. See Fig. 2.4

Table 1
Review of work in terms of measurement and identification methodology

2.2. Criticism of the different approaches

These methods have a loading system and a measuring system that are often dissociated : the data must be synchronized. The deflection measurement is estimated from a theoretical model. There is a sensitivity on the identification of the position of the load and its direction. Some methods exist to identify the center of the wrist such as trilateration [3]. Moreover, in the case of a weight, the first axis is not under load and two test campaigns must be carried out. The approach requires several hours to have sufficient data to estimate the robot parameters. In this context, a new patented system has been designed based on the ballbar system.

3. Technical Approach and concept

3.1. Principle of a bestseller: ballbar measurement

The ballbar is a measuring device mainly used in the world of machine-tools. Measurements are made by moving a prismatic joint at low speed in order to ignore the dynamic aspects and have a very accurate estimation of the spindle position. This very simple device allows an elementary implementation to evaluate a very large number of defects on the various axes of the machine tool. The implementation of such a system on a robot could be complex. First of all, the measuring range is small compared to the working space of the robot which can be about 2m. On a cartesian machine, the ballbar allows the identification of two axes simultaneously on a plane. However, for a robot, setting up a test in a plane is not suitable because all the axes will be solicited. However, the idea of loading 2 robot axes at the same time seems relevant in order to evaluate the health of specific actuators for example. Moreover, the identification

of the system is essential and requires to have enough data to estimate the parameters allowing to properly estimate the robot behavior.

3.2. Requirement specification

In order to design a metrological device for robot identification, we considered the following specifications :

- Identification of heavy robot with large workspace (>1m50) and high payload (>150kgs)
- Synchronized number of axes for robot defect observation : 2 axis at least (saddle trajectory)
- Quality of the reference frame : fixed on the ground
- Dimension of the task to be observed : 6 dimensions
- Quality of the loading force : in the two directions (push and pull)

Concerning the performances of the robot, the specifications are :

- Accuracy of the system : below 0.2mm
- Repeatability of the system : below 0.1mm
- Variation of robot positioning/deflection: over several tens of millimeters under 2500N
- Measurement quality of the force : a few newtons

3.3. Discussion about the design

The simplest solution is to connect the robot to a line between the robot end effector and the floor. From then on, the SPS (Spherical Joint (3DoFs) - Prismatic Joint (1 DoFs) and Spherical Joint (3DoFs)) solution appears, but it needs to be simplified as it is redundant of order 1. The Spherical joint can correspond to the series of 3 Revolute joints (R) whose axes of rotation converge at a point. In our application, we have decomposed our Spherical joint (S) into an Universal joint (U) and a Revolute joint (R) whose axes remain coincident with the center of the Universal joint (U). We are looking to perform measurements on large and heavy industrial robots. We limit the radius of the sphere to about 1m. The angles should cover a half-sphere. The accuracy of the sensors therefore depends on the position of the measurement on the device. Indeed, the measurement of an angle at the base of the mechanism used to calculate the position of the end effector will be higher than that used to define the orientation of the end effector at the end of the arm. One can quickly estimate the order of magnitude needed for the sensors based on their position and the angle at the base of the device. In this way, we define 4 cases, see Tab. 2 and Fig. 3. The first case takes into account a low accuracy on each Revolute joint (R) of the Universal joint (U). The second case takes into account a high accuracy for each Revolute joints. The third one considers a high accuracy at the base of the equipment. Finally, the last one simplifies the architecture to avoid redundant architecture considering an Universal Joint at the basis instead of a spherical one. The parameters of the model used for this study are the final dimensioning. At last, we define the accuracy as the ratio of cost based on the encoders in the Tab. 3. To reach an optimal configuration in terms of accuracy regarding cost, a study is performed where it is assumed that the accuracy reached by the system follows a normal centered distribution with a standard deviation equal to the accuracy divided by 2. Monte Carlo type study is played with 10^6 runs. The probability distribution model chosen is of "gamma" type (Eq.1 and 2).

$$f(x|a,b) = \frac{1}{b^a \Gamma(a)} x^{a-1} e^{\frac{-x}{b}} \tag{1}$$

where

$$\Gamma(x) = \int_0^\infty e^{-t} t^{x-1} dt \tag{2}$$

Fig. 4 presents the accuracy which can be expected. On the abscissa axis, we find the error in μm and in ordinate, the frequency normalizing the set to 1. For each model, in continuous line, we find the raw data and in dotted line the model estimates the values of the Tab. 4. The second case is the more accurate but the more expensive as well. The forth case is chosen as it divides the price of sensors by 2 and it highlights an inaccuracy up to 23% regarding the best one.

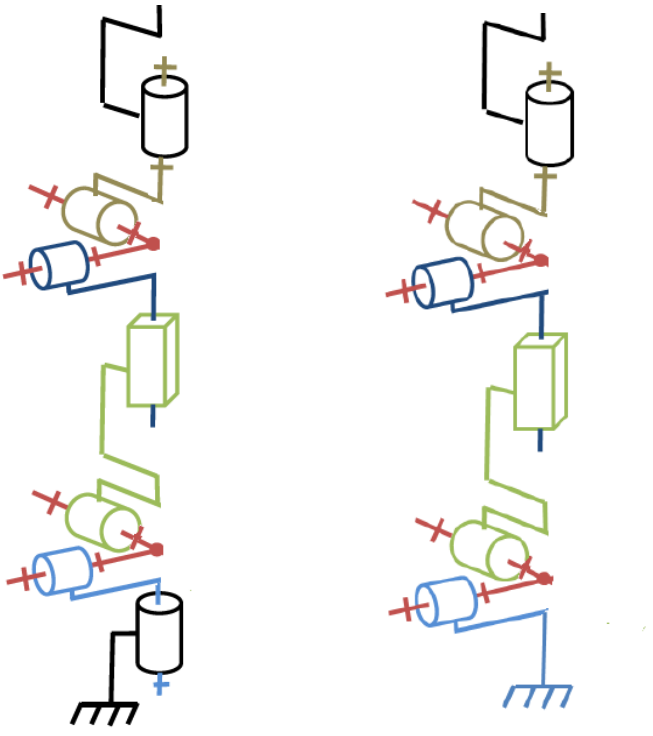

Figure 3: Studied architecture : RRRPRRR(Case I to III) - RRPRRR (Case IV) - R means Rotoïd and P Prismatic

	Type	Acc.	Type	Acc.	Type	Acc.
I	RRR	Low	P	High	RRR	Low
II	RRR	High	P	High	RRR	High
III	RRR	High	P	High	RRR	Low
IV	RR	High	P	High	RRR	Low

Table 2
4 configurations to be studied in terms of accuracy;

Sensor	Accuracy	Ratio of cost
Encoder Low accuracy	20"	1
Encoder High Accuracy	5"	4
Glass ceramic ruler Zerodur	3μm	2

Table 3
Accuracy regarding cost for encoders and glass ceramic ruler

3.4. Accessibility analysis

The universal joint orientation has an impact on the preferred test area to be carried out. To validate our design, we calculate the value of the manipulability index discretizing the workspace on the surface of a sphere with a diameter of 2m. The values obtained are then classified into 3 groups (red, violet and green) where the green colour represents the best values [19]. Fig. 5.A and Fig. 5.B present the results with a first link that can be horizontal or vertical respectively.

In the case of the first mechanism (Horizontal), a preferential measuring area is located at the center of the device while the second is located at the periphery of the mechanism. Therefore, regarding the ballbar's requirements, the configuration with a first link to be horizontal is chosen (obvious choice).

Model	Mean(μm)	Variance	a	b	Cost
I	61.05	1331	2.61	23.37	8
II	15.3	83.2	2.62	5.83	26
III	20.01	137.6	2.69	7.42	15
IV	**18.89**	126.5	2.64	7.15	**13**

Table 4
Results highlighting accuracy and cost. Model IV is chosen

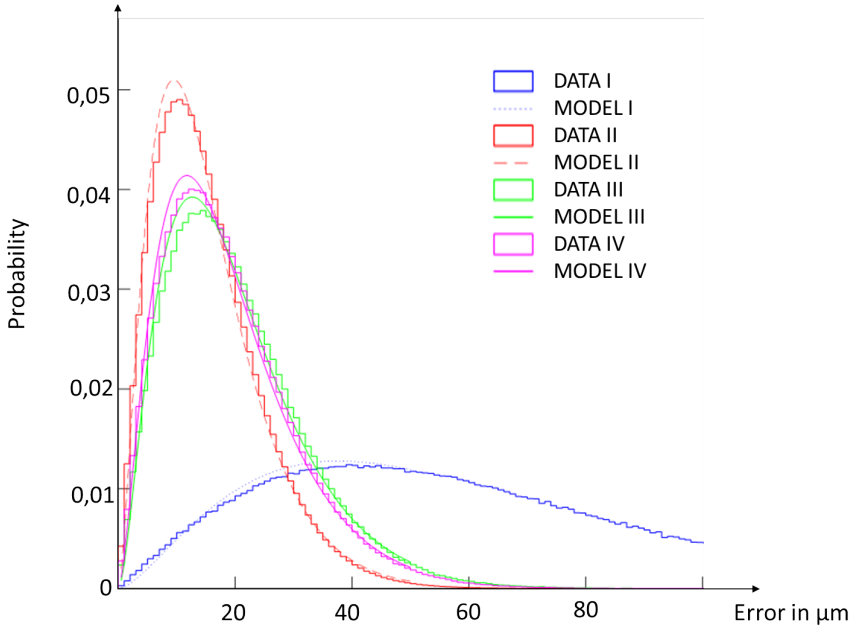

Figure 4: Architecture regarding Accuracy

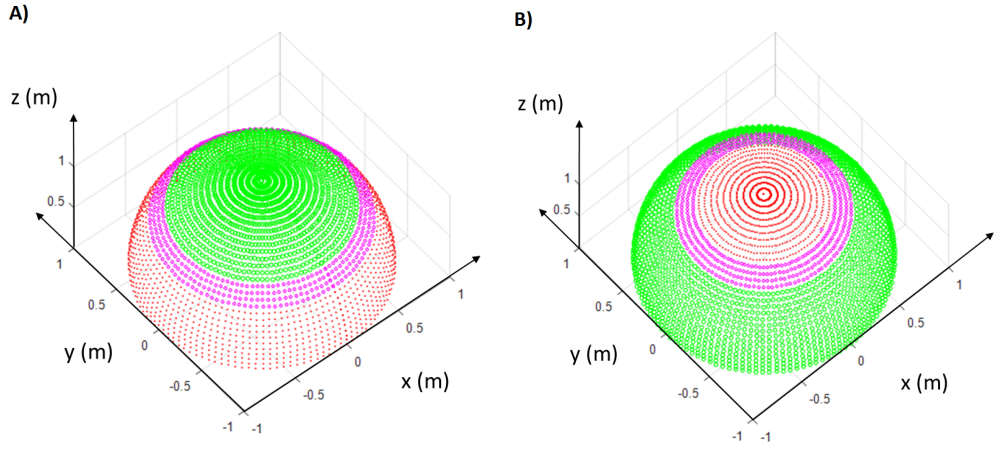

Figure 5: Manipulability criteria for the first link in horizontal (A) and vertical position(B) - Configuration A is chosen

3.5. Concept

The final mechanism is a UPUR mechanism (Universal joint (2 revolute joints) - Prismatic joint - Universal (2 revolute joints) - Revolute joint). The mechanical structure of the device is shown in Fig. 6.

Figure 6: UPUR to sollicitate industrial robot

This equipment includes a base link, a universal passive joint described by two elementary revolute joints, a linear actuator (SMC double acting pneumatic cylinder MGP series), a Universal passive joint described by two elementary Revolute joints, a Revolute passive joint providing rotation to end effector. The system is installed with the following seven sensors: two absolute encoders for the first Universal joint (Heidenhain RCN 2310), a positioning sensor for prismatic joint (Heidenhain LIC 4003), a force sensor for measuring the force (HBM U9C), two absolute encoders for the second Universal joint (Heidenhain ROC 437F). A human-machine interface (HMI) (Fig. 7) has been developed allowing the display and acquisition of measured quantities (angles, distance, force) through Labview. The interface helps deducing the positions and orientations of the upper plate center connected to the robot. The HMI allows the acquisition of static points at the request of the operator or from a trigger programmed on the robot. The information about the recorded points is displayed in a point table and can be exported in ASCII format. For each position, synchronized force and position data are recorded. The software also allows to launch continuous acquisitions with a sampling rate of one millisecond. In the case of continuous acquisition, to optimize performance, the display of the 3D device and the table of recorded points is disabled. During continuous acquisition, the data is stored in a buffer memory. At the end of the recording, the export function is automatically started. The operator must select a path to save the ASCII file with the same information as before.

4. Analysis, identification and performances of the system

A general approach to identifying a robot, whether geometric, elastostatic, kinematic or dynamic, is to compare the acquisition of data by an external sensor of known accuracy and then use these data to identify parameters using a

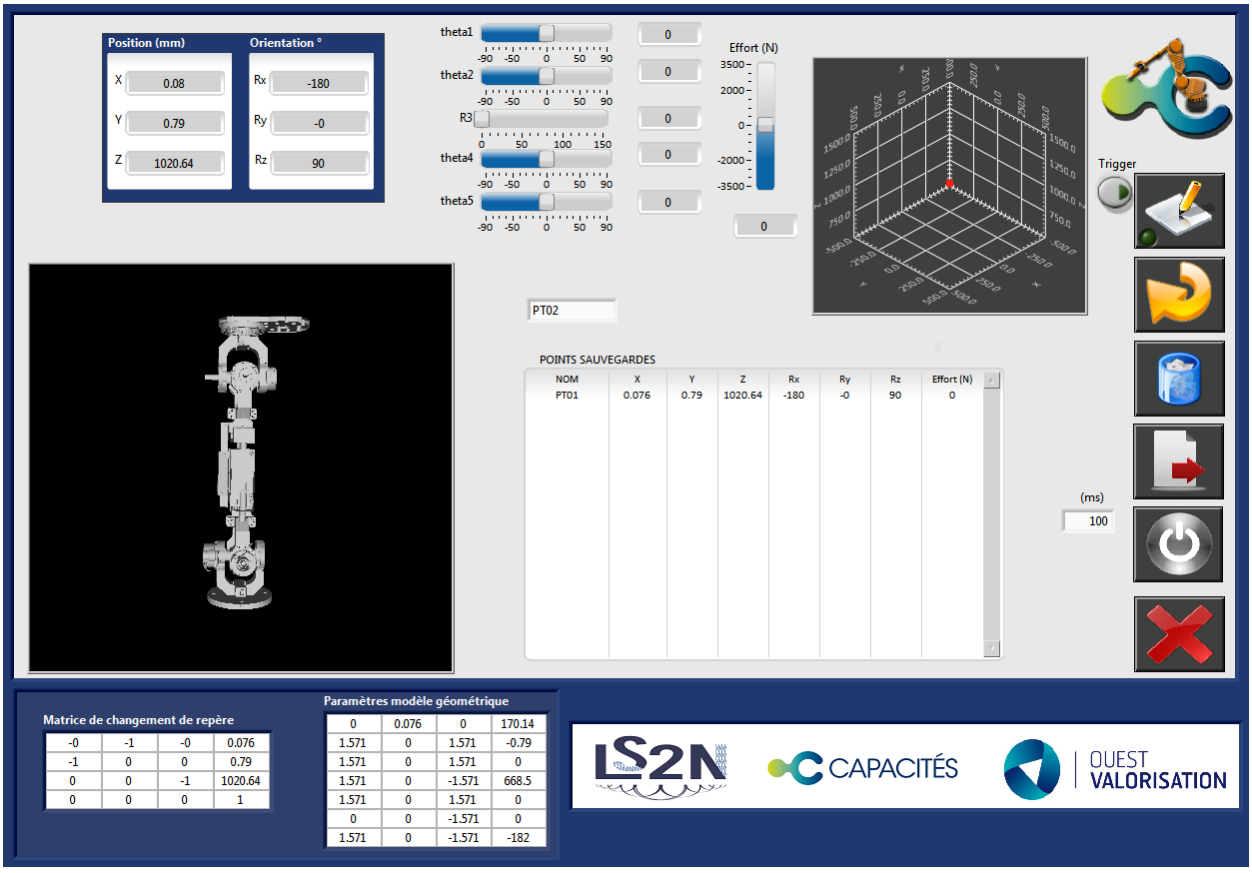

Figure 7: Human Machine Interface to synchronize data in terms of force and position colorblack

model fitting algorithm. The device used for data acquisition is a laser tracker. This involves installing a laser tracker and measuring the position of the end-effector using reflectors namely here T-MAC. This method is frequently used in industry. The visibility of the reflectors by the laser tracker is very important to obtain substantial readings. This imposes constraints on the robot end-effector path, as the reflector installed at the end-effector must be fully visible to the laser tracker in order to obtain satisfactory readings. As our system is a mechanical system, its design, geometry and mechanical properties are inacurate with respect to the theoretical model (CAD), which is considered geometrically perfect. It is therefore necessary to identify the parameters of the system to evaluate its overall accuracy.

In order to identify the equipment, a Denavit-Hartenberg Modeling (DHM) [20] is performed. The transition from frame R_{j-1} to frame R_j is expressed as a function of the following four parameters.

- α_j : angle between Z_{j-1} and Z_j, corresponding to a rotation between X_{j-1}
- d_j : distance between Z_{j-1} and Z_j along X_{j-1}
- θ : angle between X_{j-1} and X_j, corresponding to a rotation between Z_j
- r_j : distance between X_{j-1} and X_j along Z_j

The transformation matrix defining the frame R_j in the frame R_{j-1} is given by :

$$ {}^{j-1}T_j = \begin{bmatrix} cos(\theta_j) & -sin(\theta_j) & 0 & d_j \\ cos(\alpha_j)sin(\theta_j) & cos(\alpha_j)cos(\theta_j) & -sin(\alpha_j) & -r_j sin(\alpha_j) \\ sin(\alpha_j)sin(\theta_j) & sin(\alpha_j)cos(\theta_j) & cos(\alpha_j) & r_j sin(\alpha_j) \\ 0 & 0 & 0 & 1 \end{bmatrix} $$

j	α_j	d_j	θ_j	r_j	Offset
1	0	0	0	170	0
2	$\pi/2$	0	θ_1	0	$\pi/2$
3	$\pi/2$	0	θ_2	0	$\pi/2$
4	$\pi/2$	0	0	r_3+668.5	-$\pi/2$
5	$\pi/2$	0	θ_4	0	$\pi/2$
6	0	0	θ_5	0	$\pi/2$
7	$\pi/2$	0	θ_6	-182	-$\pi/2$

Table 5
Theoretical DHM parameters for the system

The system is now set up (Fig. 8). The geometrical target values coming from CAD model are entered in the Tab. 5.

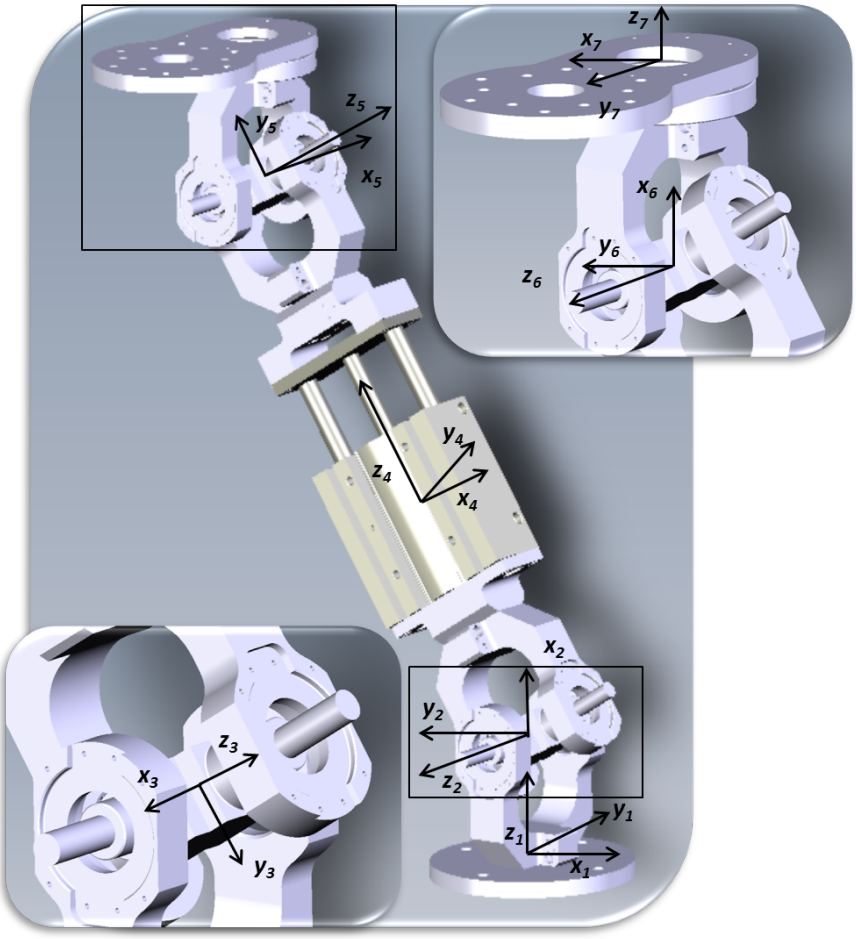

Figure 8: Positioning of the various frames regarding [20]

4.1. Performance analysis of the system

In order to obtain the measurement accuracy of the prototype (trueness and repeatability), a load qualification test is carried out during which the TCP coordinates of the robot are measured. The results obtained by the system are then compared with those measured by a metrological tool known for its accuracy and repeatability, a LEICA laser tracker. For this purpose, a robot cell equipped with a KUKA KR270 robot is used. The qualification protocol is broken down as follows:

- Realization of an empty trajectory, with stops on 30 measuring points,
- Recording of the TCP coordinates on 30 points by the device and the laser tracker,
- Achieving the same trajectory under load,
- Recording of the TCP coordinates on 30 points by the device and the laser tracker,
- Comparison of the relative movements of the TCP over 30 points
- Analysis of the measurement accuracy of the device.
- Several levels of solicitation will be performed pushing and pulling mode with 1000N and 2500N

We observe mainly T-Mac Base frame to study the performance of the system regarding repeatability and accuracy (Fig. 9). The qualification path consists of 30 measuring points (Fig. 10). The robot executes this trajectory at a constant linear speed of 0.1m/s, with a 5-seconds stop at each point to allow stable coordinate acquisition.

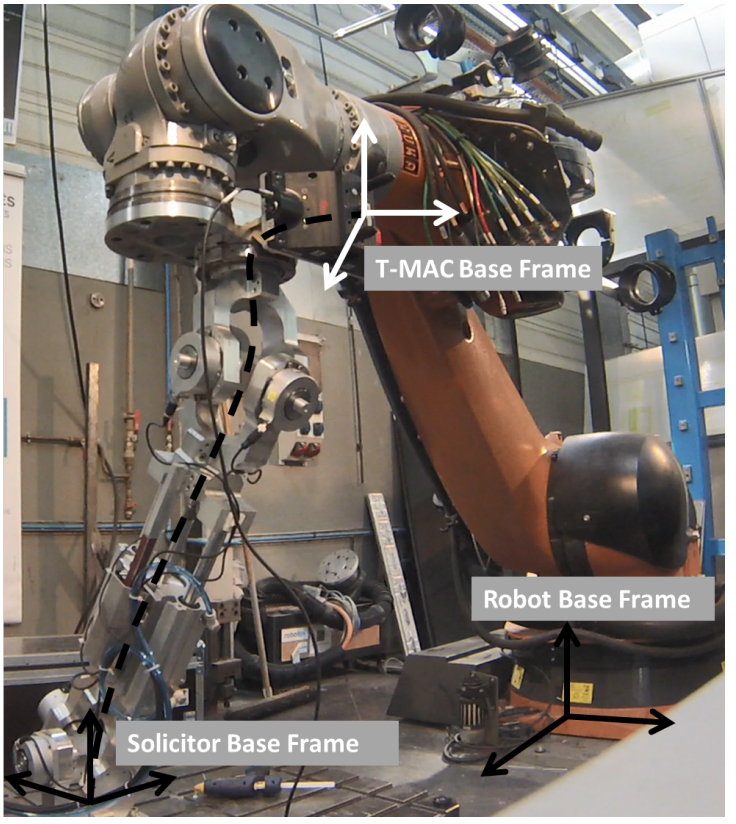

Figure 9: Trajectory in a plane of Radius 400mm

4.1.1. Repeatability measurement

Measurement repeatability is evaluated while trajectories are played 5 times consecutively. Measurement repeatability is calculated at each position using the standard formula. This repeatability is due to both the robot positioning repeatability and the measurement repeatability. Articular repeatability of the system is studied with and without load. To begin, a modeling is performed taking into account the real positioning of the various joint regarding each others. After evaluation of the DHM parameters see Tab. 6, we obtain all the defect of our device due to manufacturing and assembling. We therefore compare the repeatability measured with the device regarding that measured with the laser tracker. Tab. 7, Tab. 8 and Tab. 9 present our results and highlights that our system repeatability is under 0.03mm

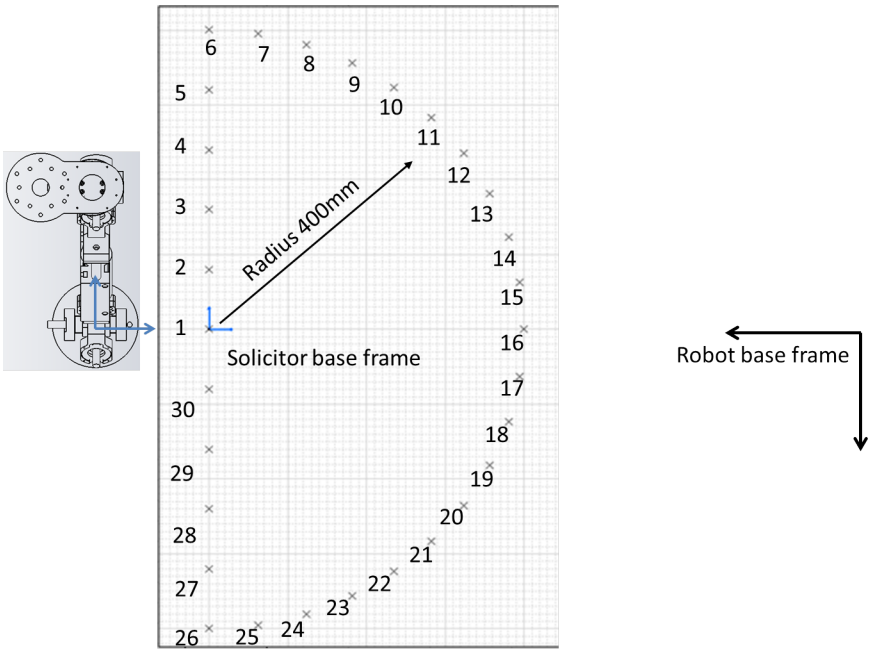

Figure 10: 30 positions on a radius 400mm

j	α	d	θ	r	Offset
1	-0.0007	0.00016	-0.0011	168.18	0
2	1.570	-0.00014	$\theta 1$	-0.720	1.57045
3	1.570	0.0001	$\theta 2$	-0.00012	1.576
4	1.570	-3.39E-5	0	$r3 + 667.039$	-1.57
5	1.595	-0.0001	$\theta 4$	0.00023	1.566
6	-0.000	0.0003	$\theta 5$	-0.0002	1.56706
7	1.567	0.00068	$\theta 6$	-185.05	0

Table 6
Evaluation of DHM parameters

	Average Repeatabilty		Maximum Repeatabilty	
	0	1KN	0	1KN
$\theta 1$	0.0011	0.0025	0.0028	0.0068
$\theta 2$	0.0010	0.0022	0.0037	0.015
$r3$	0.015	0.045	0.033	0.12
$\theta 4$	0.0028	0.0056	0.014	0.053
$\theta 5$	0.0020	0.0062	0.0037	0.016

Table 7
Articular trueness trial on an industrial robot KR270 with a laser tracker

without loading and below 0.09mm with 1kN loading. The robot's positioning repeatability measured with the device is therefore very close to that measured by the laser tracker. The first two points of the series loaded at 1kN have a fairly high repeatability, visible to both the tracker and the device. This study allows us to validate the capability of measurement of the device regarding traditional measurements via Laser Tracker.

Sollicitor	Av. Repeatabilty		Max. Repeatabilty	
	0	1KN	0	1KN
3D (mm)	0.014	0.032	0.028	0.089

Table 8
3D trueness trial on an industrial robot KR270 with a laser tracker

Tracker	Av. Repeatabilty		Max. Repeatabilty	
	0	1KN	0	1KN
3D (mm)	0.019	0.035	0.034	0.115

Table 9
3D Trueness trial on an industrial robot KR270 with a laser tracker with optimization of DHM parameters

4.1.2. Accuracy under loadings

Our objective is to validate the performance of our system to give the position of T-MAC reference frame in comparison with the laser tracker. Two configurations are tested : while pushing and while pulling with 1000N and 2500N. Without correction model, it can be observed some differences highlighting the additional work that will be needed to identify industrial robot under stress meaning while pushing or pulling it with this device (Fig. 11). While the behavior of the prismatic joint seems to be well understood, we performed a finite element analysis of the Universal joint to see its behavior under load. The software 3D Experience is used with the following boundary conditions: the use of an aluminum alloy and a force of 2500N oriented towards the center of the Universal joint, the fact of ensuring that the mesh size has a small influence on the results given by the software, the consideration of different conditions for the modeling of the assembly (global contact, use of connectors). As a result, a deformation of the base is observed (deformation between Frame 1 and Frame 2 of Fig.8) which must be taken into account in the model and which is not previously identified. Preliminary results are presented (Fig.13) and show a correlation between the offset between the tracker and the device measurements and the positioning of the lower Universal joint. Our future work will be focused on the implementation of the FEA analysis inside the software to be able to study the behavior of an industrial robot under stress without being disturbed by the device behavior.

5. Conclusion and perspectives

This paper highlights the performance of a new patented system to apply a wrench and to measure the key elements to improve robot performance in terms of accuracy under load. This system is a newer technology that is efficient, easier to use and must provide all the requisite of calibration in one system. The dynamic loader allows the positions of a robot in the workspace to be measured very quickly for different loading cases. Indeed, the measurement of the 30 positions for the 5 loading cases and with repeatability (i.e. 390 measurement points) took less than one hour. For comparison, with the tracker method previously used for elastostatic identification of robots, one day was needed to measure 30 positions for 30 robot joint configurations with only two loading cases. This device is really interesting for industrial applications based on the installation time. Moreover, we can evaluate easily the robot health evaluating the deviation of its accuracy/unaccuracy during defined period. Moreover, this allows us to make decoupled identifications (2 axes by 2 axes) whereas the literature generally proposes a global identification of all the parameters. We have highlighted in past work [3], the importance for example of identifying the first 3 axes stiffnesses of the robot from that of the wrist because there is a factor of 10 on the values to identify. Perspectives will be dedidated to the identification under load of this device. Increasing its accuracy by solving problems in geometry and mechanical responses, hence becomes a research topic for our research activities.

References

[1] Alexandr Klimchik, Alexandre Ambiehl, Sébastien Garnier, Benoit Furet, and Anatol Pashkevich. Efficiency evaluation of robots in machining applications using industrial performance measure. *Robotics and Computer-Integrated Manufacturing*, 48:12–29, 2017.

[2] Claire Dumas, Stéphane Caro, Sébastien Garnier, and Benoît Furet. Joint stiffness identification of six-revolute industrial serial robots. *Robotics and Computer-Integrated Manufacturing*, 27(4):881–888, 2011.

[3] Alexandre Ambiehl, Sébastien Garnier, Kévin Subrin, and Benoit Furet. New method for decoupling the articular stiffness identification:

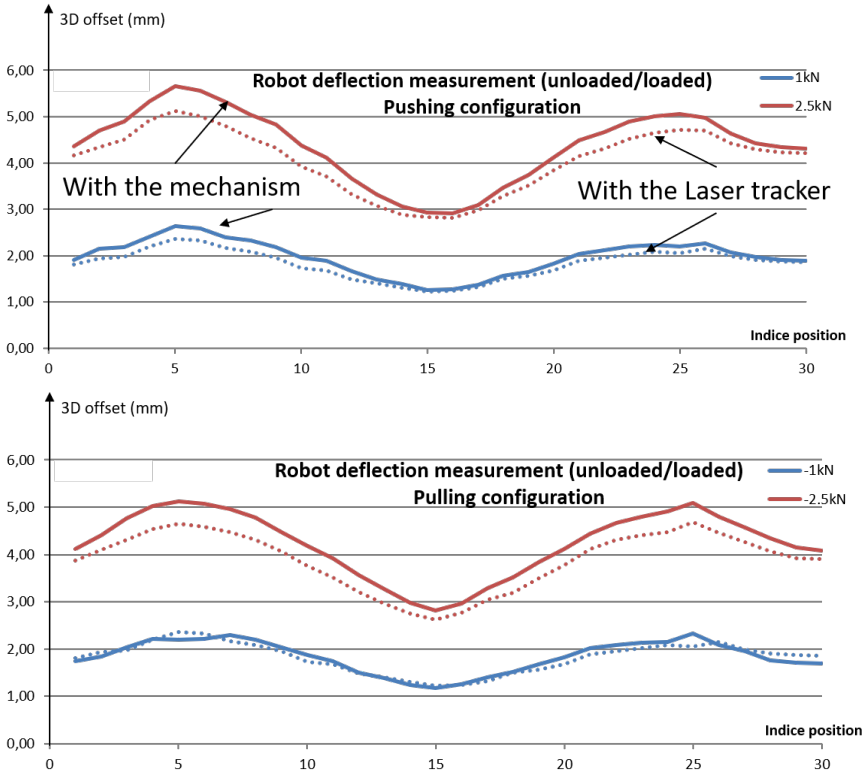

Figure 11: Robot deflection measurement with push and pull movement with 1000N and 2500N

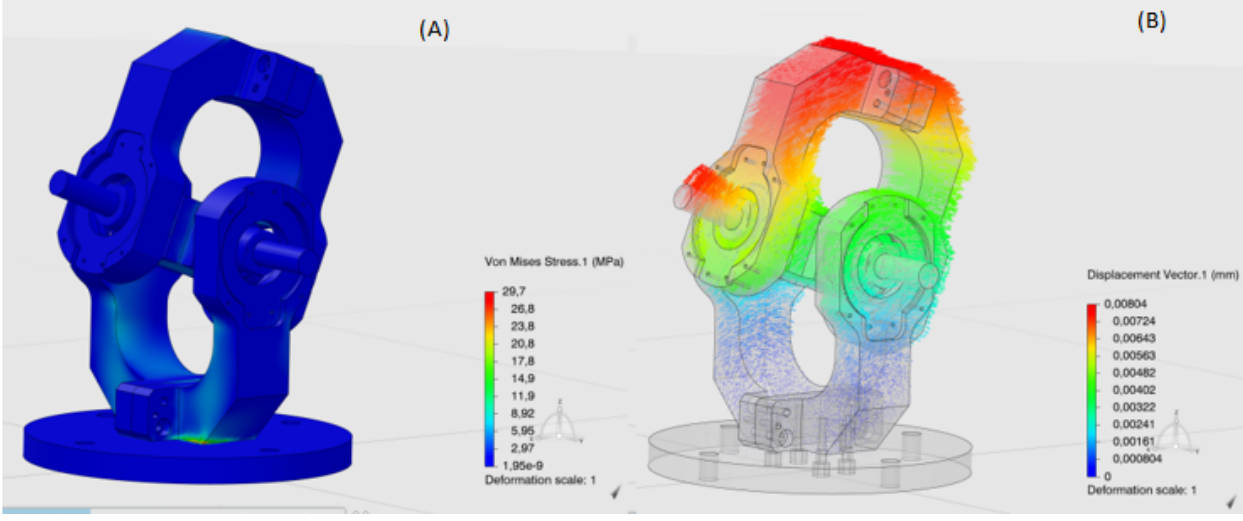

Figure 12: Finite Element Analysis of the system basis at Position 3 - Von Mises stresses (A) - Displacement vector (B)

Application to an industrial robot with double encoding system on its 3 first axis. In *2017 IEEE/RSJ International Conference on Intelligent Robots and Systems (IROS)*, pages 1478–1483. IEEE, 2017.

[4] Nikolas A Theissen, Theodoros Laspas, and Andreas Archenti. Closed-force-loop elastostatic calibration of serial articulated robots. *Robotics and Computer-Integrated Manufacturing*, 57:86–91, 2019.

[5] Yier Wu, Alexandr Klimchik, Stéphane Caro, Benoît Furet, and Anatol Pashkevich. Geometric calibration of industrial robots using enhanced partial pose measurements and design of experiments. *Robotics and Computer-Integrated Manufacturing*, 35:151–168, 2015.

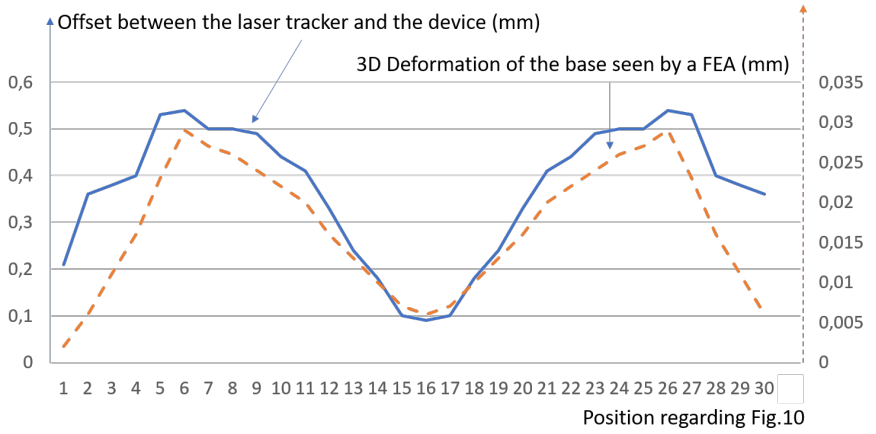

Figure 13: Correlation between the deformation of the device base seen by the laser tracker/device and the Finite Element Analysis of the base

[6] Kaveh Kamali and Ilian A Bonev. Optimal experiment design for elasto-geometrical calibration of industrial robots. *IEEE/ASME Transactions on Mechatronics*, 24(6):2733–2744, 2019.

[7] David Guérin, Stéphane Caro, Sébastien Garnier, and Alexis Girin. Optimal measurement pose selection for joint stiffness identification of an industrial robot mounted on a rail. In *2014 IEEE/ASME International Conference on Advanced Intelligent Mechatronics*, pages 1722–1727. IEEE, 2014.

[8] Christopher W Kennedy and Jaydev P Desai. Modeling and control of the mitsubishi pa-10 robot arm harmonic drive system. *IEEE/ASME Transactions on mechatronics*, 10(3):263–274, 2005.

[9] Alexander Klimchik and Anatol Pashkevich. Robotic manipulators with double encoders: accuracy improvement based on advanced stiffness modeling and intelligent control. *IFAC-PapersOnLine*, 51(11):740–745, 2018.

[10] Alexandr Klimchik, Stéphane Caro, Yier Wu, Damien Chablat, Benoît Furet, and Anatol Pashkevich. Stiffness modeling of robotic manipulator with gravity compensator. In *Computational Kinematics*, pages 185–192. Springer, 2014.

[11] Michael Ruderman, Frank Hoffmann, and Torsten Bertram. Modeling and identification of elastic robot joints with hysteresis and backlash. *IEEE Transactions on Industrial Electronics*, 56(10):3840–3847, 2009.

[12] PS Shiakolas, KL Conrad, and TC Yih. On the accuracy, repeatability, and degree of influence of kinematics parameters for industrial robots. *International journal of modelling and simulation*, 22(4):245–254, 2002.

[13] ISO NORM and EN ISO. 9283 (1998). *Manipulating industrial robots performance and criteria. Norm, EN ISO*, 9283, 1998.

[14] Andreas Archenti, Mihai Nicolescu, Guillaume Casterman, and Sven Hjelm. A new method for circular testing of machine tools under loaded condition. *Procedia CIRP*, 1:575–580, 2012.

[15] Albert Nubiola and Ilian A Bonev. Absolute robot calibration with a single telescoping ballbar. *Precision Engineering*, 38(3):472–480, 2014.

[16] Albert Nubiola, Mohamed Slamani, Ahmed Joubair, and Ilian A. Bonev. Comparison of two calibration methods for a small industrial robot based on an optical cmm and a laser tracker. *Robotica*, 32(3):447–466, 2014.

[17] Alexandre Filion, Ahmed Joubair, Antoine S Tahan, and Ilian A Bonev. Robot calibration using a portable photogrammetry system. *Robotics and Computer-Integrated Manufacturing*, 49:77–87, 2018.

[18] Claire Dumas, Stéphane Caro, Mehdi Cherif, Sébastien Garnier, and Benoît Furet. Joint stiffness identification of industrial serial robots. *Robotica*, 30(4):649–659, 2012.

[19] Peter I Corke. A robotics toolbox for matlab. *IEEE Robotics & Automation Magazine*, 3(1):24–32, 1996.

[20] Wisama Khalil and Etienne Dombre. *Modeling, identification and control of robots*. Butterworth-Heinemann, 2004.

Graphical Abstract

A metrological device for robot identification

Sebastien Garnier, Kevin Subrin

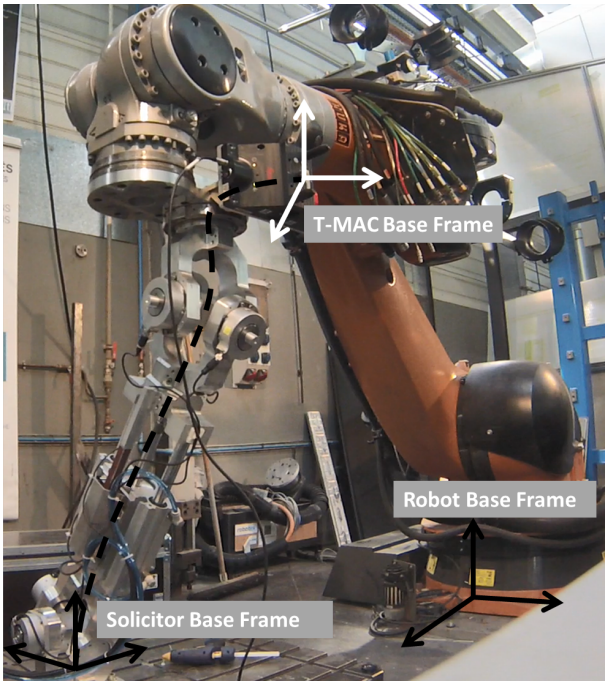

Highlights

A metrological device for robot identification

Sebastien Garnier, Kevin Subrin

- Methodology for designing a metrological device for robot performance improvement.
- Metrological device for both loading an industrial robot (up to 2500N) and measuring its deformation.
- Finite Element Analysis to understand the system behavior under stress.
- Validation test of the repeatability of the device.